Multi phonon (multiphonon) anharmonicity of MgO

Paola Giura, Lorenzo Paulatto, Fei He, Ricardo Lobo, Alexei Bosak, Eugenio Calandrini, Luigi Paolasini, Daniele Antonangeli

Multiphonon anharmonicity of MgO

Paola Giura[1], Lorenzo Paulatto[1], Fei He[1], Ricardo P. S. M. Lobo[2,3], Alexei Bosak[4], Eugenio Calandrini[5], Luigi Paolasini[4], Daniele Antonangeli[1].

[1] *Institut de minéralogie, de physique des matériaux et de cosmochimie (IMPMC), Sorbonne Université, UMR CNRS 7590, Museum National d'Histoire Naturelle, IRD UMR 206, 4 place Jussieu, F-75005 Paris, France*

[2] *LPEM, ESPCI Paris, PSL Univeristy, CNRS, F-75005 Paris, France*

[3] *Sorbonne Université, CNRS , LPEM, F-75005 Paris, France*

[4] *European Synchrotron Radiation Facility (ESRF) – ESRF – 6 rue Jules Horowitz BP220 38043 GRENOBLE CEDEX, France*

[5] *Synchrotron Soleil, L'Orme des Merisiers Saint Aubin, BP 48 91192, Gif-sur-Yvette, France*

ABSTRACT

The anharmonic lattice dynamics of MgO has been studied at ambient conditions and at high temperatures by infrared spectroscopy and inelastic X-rays scattering measurements combined with density functional perturbation theory calculations. The agreement between the measured phonon energies and widths with ab-initio calculated values provides a direct and pertinent test of the validity of advanced theoretical methods. Long observed anharmonic features in the infrared reflectivity find a clear explanation in terms of well-defined multi-phonons scattering processes and lattice dynamics peculiarities, also responsible of a significant and sharp reduction of the longitudinal optical phonon lifetime at critical finite wave vectors.

Our work highlights the importance of multi-phonons scattering processes on collective dynamics and related materials properties.

The importance and effectiveness of a synergetic approach combining experiments and ab-initio simulations to understand the complex phenomena that control the properties of materials under extreme thermodynamic conditions cannot be overstated. This joint effort becomes essential for acquiring knowledge of, and correctly modeling, the anharmonic effects on the collective dynamics of crystalline solids. Phonons anharmonicity is a very important topic of fundamental interest, also crucial on applied basis, as phonons play a major role in many physical properties such as thermal and electrical conductivity, or superconductivity.

During the past two decades theoretical and numerical tools have improved dramatically (e.g. [1, 2, 3]), allowing the simulation of anharmonic phenomena, such as phonon lifetimes and lattice thermal conductivity. This led to important applications in the study of thermoelectricity [4, 5]. Indeed knowing how the heat flows, or dissipates, is of primary importance in the conception of new and improved thermoelectric devices. More generically, the influence of multi particle coupling has been largely highlighted in a variety of materials going from those of technological interest like the thermoelectrics Bi_2Te_3, PbTe, to the alkali halides or simple metals such as aluminum [6, 7, 8, 9]. In a similar manner, calculations of the lattice thermal conductivity at high pressures and high temperatures have been carried out for many compounds of geophysical interest such as MgO [10] and $MgSiO_3$ [11], as the relative importance of heat transport mechanisms (conduction vs. radiation vs. convection) strongly influences the planet internal dynamics [12].

However, the pertinence of such approach has been challenged, in absence of an advanced description (and the consequent modeling) of the normal modes anharmonic interactions responsible of the thermodynamic behavior of crystals [13]. The way in which phonons interacts has a non-neglegible impact on the physical properties of the material, and the concept of phonon itself finds its limits.

Noteworthy, such an intense and diversified research is mostly based on computational studies. Only few are the experiments and even fewer, the studies in which the theoretical predictions and measurements are directly compared [14, 15, 9, 16, 17, 18, 19]. Macroscopic quantities, such as thermal conductivity or thermo-electric figure of merit ZT, depend on the entire phonon spectrum and are very sensitive to the approximations used in the ab-initio simulations and to the specific characteristics of individual samples (degree of crystallinity, presence and nature of defects etc.), making any comparison

difficult to interpret. From an experimental standpoint several spectroscopic techniques are necessary to probe phonons over the entire dispersion: visible (Raman, Brillouin) and infrared spectroscopies at vanishing crystal momentum, and inelastic neutrons or x-rays scattering at finite wave vector.

In this context we undertook a complete experimental and computational study on the rock-salt compound MgO, so to directly and unambiguously assess the quality of theoretical simulations of the anharmonic phonon dynamics. The choice of MgO is based on the availability of high quality single crystal, joint to a major geophysical interest. Moreover, anharmonic effects have been observed in the dielectric function of MgO and other cubic ionic crystals [20, 21, 22]. Specifically in these compounds, a pure harmonic scenario fails to describe the infrared reflectivity in the reststrahlen region, where an unexpected shoulder is systematically observed. This feature translates into an excess of spectral weight in the imaginary part of the dielectric function that is explained as continuous absorption produced by multi-phonon processes [20, 21, 19, 3].

From a theoretical point of view multi-phonon processes can be described by a perturbative correction to the harmonic phonon self-energy by adding terms in which three or more phonons may interact with each other while respecting the energy and momentum conservation. These corrections affect the real and imaginary part of the phonon self-energy $\Pi(\boldsymbol{q},\omega) = \mathcal{R}e\Pi(\boldsymbol{q},\omega) + \mathcal{J}m\Pi(\boldsymbol{q},\omega)$ shifting the resonance frequency by $\mathcal{R}e\Pi(\boldsymbol{q},\omega)$ and broadening the resonant line by the factor $\mathcal{J}m\Pi(\boldsymbol{q},\omega)$. Both quantities are accessible by spectroscopic experiments such as IR reflectivity and inelastic X-rays scattering (IXS). It is worth noting that IR reflectivity is particularly suitable to test the aptness of the theoretical approximations of the perturbed phonon self-energy, especially in systems where the difference in the charges carried by the ions is high enough to create a large LO-TO splitting [23]. In such compounds, the imaginary part of the dielectric function, far from the transverse phonon resonance, is dominated by the probability of the phonon decay $\mathcal{J}m\Pi(\boldsymbol{q},\omega)$.

In this Letter we present a thorough study of the optical phonon energies and lifetimes in the whole Brillouin zone of MgO single crystal as a function of temperature, by combining *ab-initio* calculations, IR reflectivity and IXS experiments. In particular, we present the first study in which the intrinsic anharmonic contributions to the normal modes energy and lifetime are systematically and directly compared to the relevant experimental quantities.

In a harmonic crystal, atoms oscillate around their equilibrium positions in a quadratic potential. As a consequence, phonons are stationary states of the ionic Hamiltonian: they have a well-defined frequency (Ω), energy ($\hbar\,\Omega$) and wavevector (**q**) and they do not interact with each other. Within this model there is no possible intrinsic dissipation mechanism to limit phonon lifetime. By solving the exact ionic Hamiltonian in perturbation theory, using harmonic phonons as basis [24] one gets, at first order, three self-energy contributions, depending on the 3rd and 4th derivative of the total energy with respect to harmonic perturbations. Only one of these terms has an imaginary part, which confers to the phonons a finite lifetime, i.e. an intrinsic linewidth:

$$\mathcal{J}m\prod_{\mu}(\boldsymbol{q},\omega) = -\frac{1}{2N\hbar^2}\sum_{\substack{\boldsymbol{q_1}\\ \boldsymbol{\mu_1\mu_2}}} \left|\Phi_{\mu\mu_1\mu_2}\left(-\boldsymbol{q},\boldsymbol{q_1},\boldsymbol{q}-\boldsymbol{q_1}\right)\right|^2 \times F\left(\omega,\omega_{\mu_1}\left(\boldsymbol{q_1}\right),\omega_{\mu_2}\left(\boldsymbol{q}-\boldsymbol{q_1}\right)\right), \quad (1)$$

where Φ is the matrix element governing the scattering rate of phonons with wavevectors **-q**, $\mathbf{q}_1$ and $\mathbf{q}$ $\mathbf{-q}_1$, μ_1, μ_2 are the branches indexes and *F* is defined as:

$$F(\omega,\omega_1,\omega_2) = \frac{1}{\hbar}\left[\frac{2(\omega_1+\omega_2)[1+n_B(\omega_1)+n_B(\omega_2)]}{(\omega_1+\omega_2)^2-(\omega+i\delta)^2} + \frac{2(\omega_1-\omega_2)[1+n_B(\omega_2)-n_B(\omega_1)]}{(\omega_2-\omega_1)^2-(\omega+i\delta)^2}\right], \quad (2)$$

where ω, ω_1, ω_2 are the frequencies of the phonons involved, n_B is the Bose-Einstein distribution and δ a small regularization parameter. This form ensures the conservation of energy throughout the process. Moreover, as phonons are not stationary states of the perturbative Hamiltonian, the vibrational energy spectrum, at a given **q**, is not composed by sharp energy lines, but it acquires a continuous weight which can be interpreted as the capacity of the crystal to resonate at given wavelength and energy, or, in other terms, as the rate at which the crystal can adsorb and thermalize an external perturbation. This spectrum is, at net of some structure and form factors, what is measured in infrared spectroscopy or IXS experiments. It is then possible to compute the expected measured spectral density from the self-energy according to the formula [25, 2]:

$$\sigma(\boldsymbol{q},\omega)=\sum_{\mu}\frac{-2\hbar\Omega_{\mu}(\boldsymbol{q})\mathcal{J}m\Pi_{\mu}(\boldsymbol{q},\omega)}{\left[\hbar^2\omega^2-\hbar^2\Omega_{\mu}^2(\boldsymbol{q})-2\hbar\Omega_{\mu}(\boldsymbol{q})\mathcal{R}e\Pi_{\mu}(\boldsymbol{q},\omega)\right]^2+4\hbar^2\Omega_{\mu}^2(\boldsymbol{q})\left[\mathcal{J}m\Pi_{\mu}(\boldsymbol{q},\omega)\right]^2}\ , \quad (3)$$

where **q** and ω are the applied wavevector and frequency, μ is the phonon branch index, Ω are the harmonic phonon frequencies, Π is the self-energy of each phonon [26]. In the limit where the Π dependence on ω is very weak, this equation reduces to a linear combination of Lorentzian functions, each centered around $\Omega_{\mu}(\boldsymbol{q})+\mathcal{R}e\Pi_{\mu}(\boldsymbol{q},\omega)$ and of width $\mathcal{J}m\Pi_{\mu}(\boldsymbol{q},\omega)$. In general, the most intense peaks of $\sigma(\boldsymbol{q},\omega)$ can be unambiguously associated with the harmonic phonons. Conversely, it can occur that $\sigma(\boldsymbol{q},\omega)$ has one or more secondary peaks which cannot be associated with a single phonon. This is often the case when two broad regions of the phonon phase-space have the right energy, momentum and symmetry to concur in producing an excess of spectral weight (ESW) at a specific energy and **q**. In the following we will see the experimental evidences of this phenomenon in our IR measurement and the way in which it reflects in the IXS data.

Infrared reflectivity measurements have been carried out in the far and mid infrared range (100 ÷ 6000 cm^{-1}) at 300 and 873 K [28].

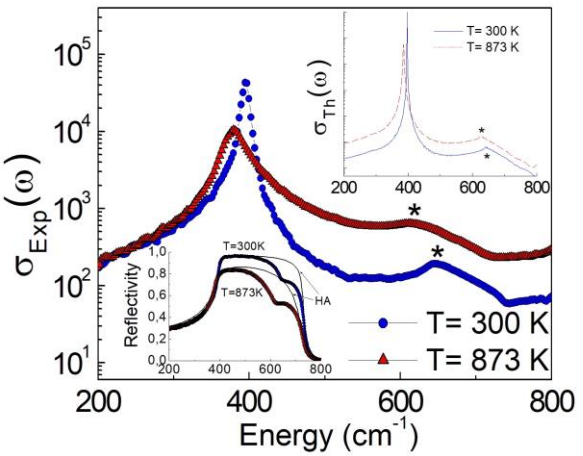

FIG. 1. . Experimental (symbols) and theoretical (lines in the upper inset) optical conductivity of MgO at 300 and 873 K. The bottom inset shows the corresponding measured infrared reflectivity spectra (symbols) together with the theoretical reflectivity foreseen in the harmonic approximation (HA) (black lines). Stars indicate the position of the ESW.

Phononic features are clearly visible in the reflectivity spectra in the range between 200 and 800 cm^{-1} (bottom inset of FIG. 1). At low energy, the reflectivity abruptly increases at the proximity of the transverse optical (TO) phonon energy as expected, reaching the reststrahlen plateau that exhibits a temperature dependent shoulder instead of ending at the longitudinal optical (LO) phonon energy as predicted by the harmonic model (thin black lines in the bottom inset of Figure 1). As already mentioned, this is not peculiar of MgO but it is observed in many rock-salt compounds and it is rationalized as the direct manifestation of the phonon-phonon coupling through anharmonic interactions [20, 25, 19]. Fig. 1 shows the optical conductivity obtained by applying the Kramers-Kronig relations to the extended reflectivity spectra and by Density Functional Perturbation Theory (DFPT) calculations. In both cases, two features are clearly visible, the most intense, at around 400 cm^{-1}, due to the TO resonance, and a second weaker one, between 600 and 650 cm^{-1}, the ESW associated to multi-phonons scattering process. The existence of a distinctly detectable ESW implies that enhanced phonon decay channels open at these specific energies, slightly lower than the one of LO phonon at Γ.

Our IXS measurements and DFPT calculations allow to better understand the origin and the implication of this decay on the phonon dispersion across the entire Brillouin zone [28].

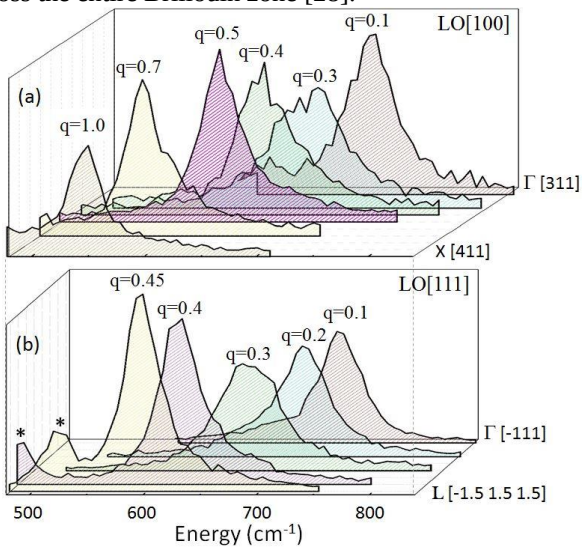

FIG. 2. Inelastic X-rays scattering spectra of the longitudinal optical phonon of MgO at 873 K along the (a) [100] and (b) [111] direction. The * indicate longitudinal acoustic phonons sometimes visible in the probed energy range.

In particular, both calculations and measurements evidence a seemingly erratic variation of the phonon widths with the wave vector, and a sharp, extremely high enlargement at wave vectors for which the LO phonon branches matches the energies of the ESW observed in infrared data. The IXS spectra obtained at

873 K for the LO branches along the [1,0,0] and [1,1,1] directions, rather than the classically expected monotonic evolution with the wave vector, show an anomalous decrease of the peak intensity accompanied by a width increase mostly pronounced at the reduced vector, q=0.3 (FIG. 2). The corresponding energy (650 cm^{-1}) is in agreement with the energy at which the maximum of the ESW is observed in the optical conductivity, arguing for a common multiphonon anharmonic mechanism for both phenomena. The origin of these anomalies becomes clear when comparing the experimental evidences to the *ab-initio* calculations.

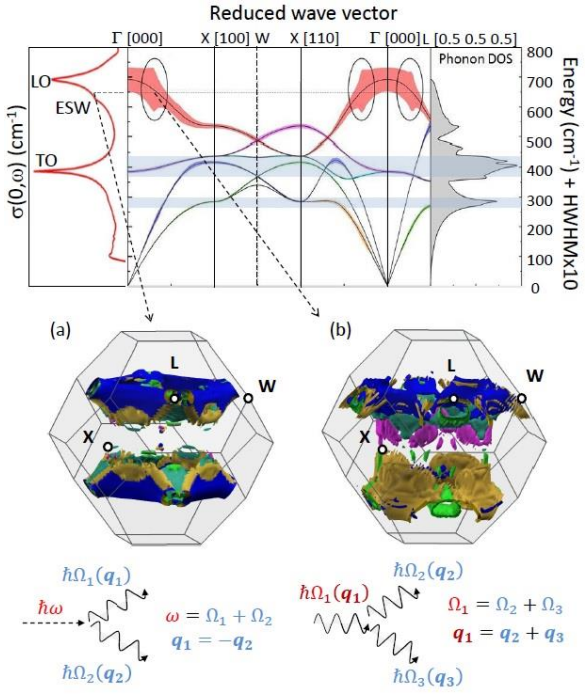

FIG. 3. Calculations of MgO phonon dispersion at 873 K along selected directions together with the phonon density of state (right panel) and the expected spectral density at Γ (left panel). The phonon branches are represented with a variable-width filled band: corresponding to the anharmonic width multiplied by a factor 10. The open dark gray circles indicate the reduced q position at which an anomalous enlargement of the phonon width is expected for the high energy LO branches. The dotted line across the LO branches is a guide for the eyes projecting at Γ the energy of the LO phonon at the q where the width exhibits the maxima. This energy matches the ESW in the computed spectral weight σ(0,ω). The shadow areas show the reciprocal space region where the phonon density of state is particularly high. (a) Final state decomposition of the ESW at Γ and (b) of the LO phonon at q = (1/4 0 0). Colored surfaces contain 10% (a), 20% (b) of the Brillouin zone volume and around 90% of the contribution to the linewidth.

FIG. 3 shows the computed phonon dispersions at 873 K along the main crystallographic directions together with the phonon density of state (right panel) and the phonon spectral weight function at Γ, σ (**0**,ω) (left panel). The phonon widths are displayed as a filled colored band superposed to the corresponding branches. In agreement with the experiments, LO phonon widths exhibit a non-smooth behavior, with a sharp increase at q=0.25 along the [100], [110] and [111] directions. This is a further independent indication of the opening of decay channels strongly affecting the phonon lifetime. As well, the energy at which the sharp increase of the LO phonon width is observed is very close to the energy of the ESW found in the imaginary part of the phonon-phonon self-energy $\mathcal{J}m\Pi_{\mu}(\mathbf{0},\omega)$.

Two different decay mechanisms are responsible for the ESW at Γ and of the anomalous intensity and width of the LO phonon at q = (1/4 0 0), but both features have a common ground: a broad, flat region in the phonon phase-space with the right energy, momentum and symmetry to allow an extended surface of final states. In the first case, the incoming photon of energy $\hbar\omega$ and $\mathbf{q} = \mathbf{0}$ decays in two phonons such that $\mathbf{q}_1 = -\mathbf{q}_2$ and the $\hbar\Omega_1 + \hbar\Omega_2 = \hbar\omega$. In the second case a three phonons process occurs, in which the LO mode at q = (1/4 0 0) decays into two others of lower energy (within the respect of the energy and momentum conservation laws). This is summarized in FIG. 3, which also illustrates the final states decomposition of the ESW at Γ (a) and of the LO phonon at q = (1/4 0 0) (b). The surfaces enclosing the phonons contributing to the two processes are represented using a color code consistent with the top panel. The total surface contains 10% of the Brillouin zone volume for the (a) process and 20 % for the (b) decay. In both cases it represents around 90% of the contribution to the linewidth.

As illustrated in FIG.4 (a) and (b), IR and IXS experiments and calculations are in an excellent agreement on phonon energies at both temperatures. This clearly demonstrates that *ab-initio* calculations within the harmonic approximation, once performed for a lattice parameters fixed to the experimental values, are able to accurately describe phonon energies at least up to here-investigated temperatures. Conversely, comparison of the measured and computed phonon widths (FIG. 4 (c)) allows for the direct assessment of the validity of the theoretical treatment of anharmonicity. The remarkable agreement clearly proves the high level of accuracy of our first principle calculations. More precisely, both experiments and calculations exhibit structured linewidth dispersion, very far from a monotonic behaviour. The existence of a sharp maximum in the

computed linewidths, there where is experimentally observed, is a strong indication of the quality of the calculations.

The non-monotonic dependence of the phonon width is the consequence of the peculiar structure of the phonon density of state (right panel in FIG. 3), which, in turn, originates from the extended flatness of several phonon branches across a large portion of the Brillouin zone (FIG. 3). Specifically, the two major peaks in the phonon density of states come respectively from the bending of the acoustic branches at the zone edges and from the non-dispersive nature of the transverse optical phonons.

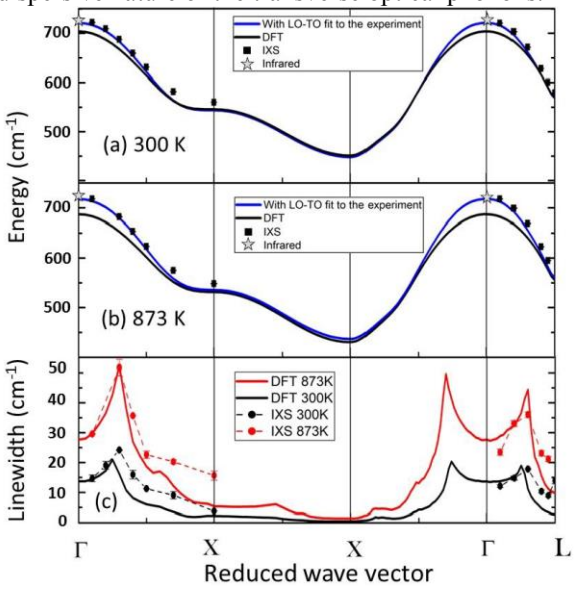

FIG.4. LO experimental (symbols) and computed (lines) energy dispersions at 300 K (a) and 873 K (b). The blue curves are results of DFPT calculations corrected by tuning the infinite value of the dielectric function to match the experimentally measured LO-TO splitting. Panel (c): the measured (symbols) and computed (lines) LO width dispersions along the main crystallographic directions at 873 K (red) and 300 K (black).

While non-dispersive optic modes are common to many non-ionic binary compounds [13], in the case of ionic systems, like MgO or the alkali halides, the strong ionic repulsion at the origin of the large LO-TO splitting, bends the dispersion of the longitudinal optical branches [27], with non-negligible consequences on the weight of the LO phonons on the thermal conductivity due to the quadratic dependence on the velocity (proportional to the slope of the energy dispersion). Contributions of LO modes might become significant especially at high temperature when the more energetic optical states start to be heavily populated. Our study shows that even in the presence of sharp optical dispersions, the existence of extended region of final states in the reciprocal space may affect the contribution of the optical modes to the thermal conductivity by the dramatic reduction of their lifetime. This highlights the importance of the correct treatment of anharmonic contributions to the thermodynamic properties of solids. It is worth to point out that the opening of strong frequency- and momentum-dependent decay channels alters, on different scale, the phonon lifetime of all the modes including the acoustic ones, and therefore must be evaluated and carefully treated.

In conclusion we report a combined experimental and theoretical study of the spectroscopic signatures of the anharmonic effects on the lattice dynamics of the binary ionic insulator MgO. The anharmonic features observed in the infrared reflectivity and systematically reported since the ‘70s in many rock salt compounds, find a common explanation to the maximum in the highly structured dispersion shown by the LO phonon widths: both the ESW at Γ and the dramatic reduction of the LO phonon lifetime at q=0.25 are due to well-identified multi-phonons scattering processes favored by the band structure peculiarities of the compound. On a more general ground, our results provide an essential benchmark for testing the validity of advanced theoretical treatment by first principle calculations.

AKNOWLEDGMENT

This work was supported by the China Scholarship Council – Sorbonne Université program for doctoral scholarships, and by the Conseil Régional d’Île-de-France through the DIM OxyMORE. HPC resources are granted under the GENCI allocation A0030907320. Femtosecond laser micro-machining at the Institute de Minéralogie de Physique des Matériaux et de Cosmochimie (IMPMC), Paris has been developed and realized by the “Cellule Project” with the financial support of ANR 2010-JCJC-604-01. E. C. acknowledges financial support from the French state funds within the framework of the Cluster of Excellence MATISSE led by Sorbonne Université. We thank M. Lazzeri for fruitful discussions.

References :

[1] S. Baroni, S. de Gironcoli, A. Dal Corso, and P. Giannozzi, *Phonons and related crystal properties from density-functional perturbation theory*, Rev. Mod. Phys. 73, 515 (2001).

[2] L Paulatto, I Errea, M Calandra, F Mauri, *First-principles calculations of phonon frequencies, lifetimes, and spectral functions from weak to strong anharmonicity: The example of palladium hydrides*, Physical Review B 91 (5), 054304 (2015).

[3] G. Fugallo, B. Rousseau and M. Lazzeri, *Infrared reflectance, transmittance, and emittance spectra of MgO from first principles*, Phys. Rev. B 98, 184307 (2018).

[4] G. Chen, T. Zeng, T. Borca-Tasciuc, and D. Song, *Phonon Engineering in Nanostructures for Solid-State Energy Conversion*, Mater. Sci. Eng. 292, 155 (2000).
[5] Q. Yin and S. Y. Savrasov, *Origin of Low Thermal Conductivity in Nuclear Fuels*, Phys. Rev. Lett. 100, 225504 (2008).
[6] N- K. Ravichandran and D. Broido, *Non-monotonic pressure dependence of the thermal conductivity of boron arsenide*, Nat. Com 10, 827 (2019).
[7] O. Hellman and D. A. Broido, *Phonon thermal transport in Bi_2Te_3 from first principles*, Phys. Rev. B 90, 134309 (2014).
[8] Z. Tian, J. Garg, K. Esfarjani, T. Shiga, J. Shiomi and G. Chen, *Phonon conduction in PbSe, PbTe, and $PbTe_{1-x}Se_x$ from first-principles calculations*, Phys. Rev. B 85, 184303 (2012).
[9] X. Tang, Chen W. Li and B. Fultz, *Anharmonicity-induced phonon broadening in aluminum at high temperatures*, Phys. Rev. B 82, 184301 (2010).
[10] N. de Koker, *Thermal Conductivity of MgO Periclase from Equilibrium First Principles Molecular Dynamics*, Phys. Rev. Lett 103, 125902 (2009).
[11] H. Dekura, T. Tsuchiya, J. Tsuchiya, Ab initio Lattice *Thermal Conductivity of $MgSiO_3$ Perovskite as Found in Earth's Lower Mantle*, Phys. Rev. Lett. 110, 025904 (2013).
[12] T. Lay, J. Hernlund and B. A. Buffet, *Core–mantle boundary heat flow*, Nature Geosci. 1, 25 (2008).
[13] A. Togo et al. Phys. Rev. B 91, *Distributions of phonon lifetimes in Brillouin zones*, 094306 (2015).
[14] P-F. Lory et al. *Direct measurement of individual phonon lifetimes in the clathrate compound $Ba_{7.81}Ge4_{0.67}Au_{5.33}$*, Nat. Comm. 8, 491 (2017).
[15] H. Uchiyama, Y. Oshima, R. Patterson, S. Iwamoto, J. Shiomi, and K. Shimamura, *Phonon Lifetime Observation in Epitaxial ScN Film with Inelastic X-Ray Scattering Spectroscopy*, Phys. Rev. Lett 120, 235901 (2018).
[16] J. W. L. Pang, W. J. L. Buyers, A. Chernatynskiy, M. D. Lumsden, B. C. Larson and S. R. Phillpot, *Phonon Lifetime Investigation of Anharmonicity and Thermal Conductivity of UO_2 by Neutron Scattering and Theory*, Phys. Rev. Lett 110, 157401 (2013).
[17] R. Pradip, P. Piekarz, A. Bosak, D. G. Merkel, O. Waller, A. Seiler, A. I. Chumakov, R. Rüffer, A. M. Oles, K. Parlinski, M. Krisch, T. Baumbach and S. Stankov, *Lattice Dynamics of EuO: Evidence for Giant Spin-Phonon Coupling*, Phys. Rev. Lett. 116, 185501 (2016).
[18] P. Giura, N. Bonini, G. Creff, J. B. Brubach, P. Roy, and M. Lazzeri, *Temperature evolution of infrared- and Raman-active phonons in graphite*. Phys. Rev. B 86, 121404(R), (2012).
[19] T. Sun, Ph B. Allen, D. G. Stahnke, S. D. Jacobsen and C. C. Homes, *Infrared properties of ferropericlase $Mg_{1-x}Fe_xO$: Experiment and theory*, Phys. Rev. B 77, 134303 (2008).
[20] J. R. Jasperse, A. Kahan, J. N. Plendl, S. S. Mitra, *Temperature Dependence of Infrared Dispersion in Ionic Crystals LiF and MgO* Phys. Rev. 146, 526 (1966).
[21] J. Breeze, Ph. D. Theses *Temperature and Frequency Dependence of Complex Permittivity in Metal Oxide Dielectrics: Theory, Modelling and Measurement*, Springer Theses (2016).
[22] G. A. Adebayo, Y. Liang, C. R. Miranda and S. Scandolo, *Infrared absorption of MgO at high pressures and temperatures: A molecular dynamic Study*, J. Chem. Phys. 131, 014506 (2009).
[23] N. W. Aschroft and N. D. Mermin, *Solid State Physics*, Holt, Rinehart and Winston, (1976).
[24] M. Calandra, M. Lazzeri F. Mauri, *Anharmonic and non-adiabatic effects in MgB2: Implications for the isotope effect and interpretation of Raman spectra*, Physica C: Superconductivity, 456, 1–2, 1 Pages 38-44, (2007).
[25] R. A. Cowley, *Anharmonic crystals*, Rep. Prog. Phys. 31, 123, (1968).
[26] As we did not include the 4-vertex term of the self-energy, which is real and typically has the opposite sign and similar magnitude to real part of the 3-vertex term, we included only the imaginary part of the self-energy in this expression.
[27] I. S. Messaoudi, A. Zaoui and M. Ferhat, *Band-gap and phonon distribution in alkali halides*, Phys. Status Solidi B 252, No. 3, 490–495 (2015).
[28] See Supplemental Material at URL……. for details concerning the infrared and IXS experiments and calculations.